

## INFLUENCE OF VEHICLE PARAMETERS ON DIRECTIONAL STABILITY DURING ELECTRIC POWERTRAIN FAULTS IN PASSENGER CARS

<sup>1</sup>Wanner, Daniel\* ; <sup>1</sup>Drugge, Lars; <sup>1</sup>Stensson Trigell, Annika

<sup>1</sup>KTH Vehicle Dynamics, Royal Institute of Technology, Stockholm, Sweden and SHC – Swedish Hybrid Vehicle Centre

KEYWORDS – Vehicle Dynamics; Vehicle Safety; Fault Tolerance; Electric Powertrain; Sensitivity Study

### ABSTRACT

Electric powertrain faults that could occur during normal driving can affect the dynamic behaviour of the vehicle and might result in significant course deviations. The severity depends both on the characteristics of the fault itself as well as on how sensitive the vehicle reacts to this type of fault. In this work, a sensitivity study is conducted on the effects of vehicle design parameters, such as geometries and tyre characteristics, and fault characteristics. The vehicle specifications are based on three different parameter sets representing a small city car, a medium-sized sedan and a large passenger car. The evaluation criteria cover the main motions of the vehicle, i.e. longitudinal velocity difference, lateral offset and side slip angle on the rear axle as indicator of the directional stability. A design of experiments approach is applied and the influence on the course deviation is analysed for each studied parameter separately and for all first order combinations. Vehicle parameters of high sensitivity have been found for each criterion. The mass factor is highly relevant for all three motions, while the additional factors wheel base, track width, yaw inertia and vehicle velocity are mainly influencing the lateral and the yaw motion. Changes in the tyre parameters are in general less significant than the vehicle parameters. Among the tyre parameters, the stiffness factor of the tyres on the rear axle has the major influence resulting in a reduction of the course deviation for a stiffer tyre. The fault amplitude is an important fault parameter, together with the fault starting gradient and number of wheels with fault. In this study, it was found that a larger vehicle representing a SUV is more sensitive to these types of faults. To conclude, the result of an electric powertrain fault can cause significant course deviations for all three vehicle types studied.

### INTRODUCTION

The electrification of chassis and driveline systems in passenger cars is beneficial for traffic safety, vehicle handling, comfort and environment. Advanced chassis systems, such as electronic stability control or semi-active suspension, assist the driver to reach its destination in a safe and comfortable manner. The former system reduces single-vehicle accidents significantly as an example (1). Electrified driveline systems have become more common in the last decade. Hybrid-electric and pure-electric driveline systems were introduced in order to fulfil legal environmental requirements of various governments and find alternative solutions due to the shortage of fossil fuels (2). The increase of electric and electronic (E/E) components results in a higher complexity of the overall vehicle system. Therefore, the probability of faults in these vehicles increases. These local faults in components can lead to global failures affecting the path of a vehicle. Faults that occur in chassis and driveline systems have different degrees of severity. They influence of the course deviation in two different aspects. First, it depends on the characteristics of the fault itself. Size, duration and form of a fault have strong influence on its severity. Secondly, other vehicle design parameters such as geometries and tyre characteristics affect the influence of a fault on the vehicle behaviour as well.

Previous research has shown that faults can have a significant influence on the course deviation. However, these studies are based merely on one set of vehicle parameters and one set of tyre characteristics (3, 4, 5, 6). Previously, the authors developed a fault classification method for passenger cars and evaluated it for one vehicle configuration (medium-sized passenger car), focusing on effects of different types of faults (5).

The aim of this study is to evaluate the influence of different vehicle parameters on the vehicle behaviour in case of a fault that affects normal driving conditions. The study covers both variations in vehicle design, such as geometries and tyre characteristics, and variations of the vehicle type. The fault itself is varied as well in order to give a more general impression on how different generic fault types act on the resulting vehicle behaviour.

## METHODOLOGY

Important vehicle parameters such as vehicle mass, centre of gravity position and tyre stiffness are selected and analysed. Relevant parameters of a fault, such as fault amplitude and fault location, are varied as well. An advanced vehicle dynamics model is used. The fault model is generic and can occur due to various reasons, for example in the field-weakening range of an electric machine of permanent magnet type. The generic fault is induced as a braking torque and directly applied on the wheel. The normal driving condition is set by a straight line driving manoeuvre. A multi-variable testing and analysis method was conducted employing the vehicle dynamics model and its generic fault model. Three different types of parameter sets were analysed individually; i.e. *vehicle*, *tyre* and *fault* parameters. The effect of each parameter set was tested for a fault on front and rear axle, respectively. Further, three different types of passenger cars are analysed, covering a broad spectrum of passenger cars. Each parameter has been analysed separately as well as all of their first order combinations. The analysis is based on three objective criteria, indicating the influence on the course deviation of the analysed parameters. The evaluation criteria cover the main motions of the vehicle, i.e. longitudinal velocity difference, lateral offset and slip angle difference as indicator of the directional stability.

### Design of experiments

This study is based on a multi-variable testing and analysis method called design of experiments; more specifically fractional factorial design (FFD) (7). The main goal is to analyse the effects of level changes for different design parameters, so called factors, and run a minimum amount of simulations according to a simulation test plan. This simulation test plan is described by an orthogonal matrix, which allows testing several factors systematically at two or more levels, without the repetition of single simulation runs. The resulting effects of the experiment can be separated into main and interaction effects. The main effect is the average change of the system's response produced by the level change of one factor. The interaction effect determines the dependency of two or more factors on each other for their simultaneous level changes.

Full factorial design replicates an experiment for a complete set of possible combinations. This method grows exponentially with the number of analysed factors  $k$  and their number of levels  $l$ , and results in a high number of simulations  $n_{sim} = l^k$ . Thus, every additional factor has to be considered wisely. In order to handle this growth in number of simulations, fractional factorial design is introduced. It reduces the number of simulations without reducing the significance of the main effects as well as low-order interaction effects. This so called scarcity of effects principle yields that certain high-order interaction effects cannot be analysed any longer. The system is likely to be driven primarily by some of the main and low-order interaction effects. In this study two levels for each factor are analysed. Equation (1) describes the main and interaction effects,  $c_{x_i}$ , with

$$c_{x_i} = \frac{\sum f(\bar{x}|_{x_i+}) - \sum f(\bar{x}|_{x_i-})}{\frac{n_{sim}}{2}}, \quad (1)$$

where  $f(\bar{x})$  is the function defining the response and  $x_i$  is the  $i$ -th factor in the vector  $\bar{x}$  containing all factors and their interactions for high (+) and low (-) levels.

### Vehicle model

In this study, an advanced vehicle dynamics model is applied, using a co-simulation environment with IPG CarMaker and Matlab/Simulink (8). The tyre characteristics are implemented with a fully parameterised Magic Formula tyre model with combined slip according to (9). A generic fault model is applied based on a previously developed fault model for an electrical driveline (5). The fault torque characteristics, such as fault torque amplitude and fault rise time, can be altered in the fault model, and are then directly applied as a braking torque on the wheel of the vehicle model. Typical faults that this model represents are an inverter-shutdown fault or a brake-system fault.

### Vehicle specifications

The vehicle specifications are based on three different parameter sets representing a *small* city car (S), a *medium*-sized sedan (M) and a *large* passenger car (L) such as a SUV. This covers a broad spectrum of the vehicle fleet worldwide. Standard components of the chassis system, i.e. friction brakes, a passive steering system and a passive suspension system, are considered. Linear springs and anti-roll bar coefficients as well as non-linear damping characteristics based on measured data are applied, see Figure 1. The three basic vehicle parameter sets are listed in Table 1. The parameters of the medium and the large vehicle are based on measured vehicle data.

The parameters of the small vehicle are estimated by using mean values of 10 city cars for mass and geometries, simple equations for the moments of inertia and similar eigen-frequencies and characteristic damping coefficient as for the medium vehicle for the suspension parameters. The selection of important vehicle parameters is based on previous studies for external disturbances and component faults (5, 10) and is shown in Table 2. The amplitude of the fault torque on the wheel is based on an electric machine fault model for the small vehicle and adapted correspondingly with average power ratios for the medium and large vehicle type.

Table 1 Setup for the three analysed vehicle types.

Vehicle parameter	Symbol	Unit	Small	Medium	Large
Vehicle mass	m	kg	900	1300	2050
Unsprung mass	$m_u$	kg	30	39	55
Body yaw inertia	$I_z$	$\text{kgm}^2$	1145	2100	4150
Body pitch inertia	$I_y$	$\text{kgm}^2$	937	2125	4100
Body roll inertia	$I_x$	$\text{kgm}^2$	305	450	775
Wheel base	l	m	2.2	2.5	2.7
Track width	s	m	1.35	1.5	1.6
Centre of gravity (CG) ratio to the front axle	$\lambda$	-	0.5	0.5	0.5
Vertical CG ratio	$\kappa$	-	0.21	0.22	0.22
Front spring stiffness	$c_1, c_2$	$\text{Nm}^{-1}$	13650	20000	36200
Rear spring stiffness	$c_3, c_4$	$\text{Nm}^{-1}$	16360	24000	39200
Front anti-roll bar stiffness	$c_f$	$\text{Nm}^{-1}$	10238	15000	11265
Rear anti-roll bar stiffness	$c_r$	$\text{Nm}^{-1}$	8180	12000	5325
Amplitude of fault torque	$T_f$	$\text{Nm}^{-1}$	215	375	775
Tyre dimensions	-	-	175/55R15	205/60R15	235/65R17
Tyre stiffness scaling factor (SF)	$\lambda_K$	-	1	1	1
Tyre peak friction SF	$\lambda_\mu$	-	1	1	1
Tyre shape SF	$\lambda_C$	-	1	1	1

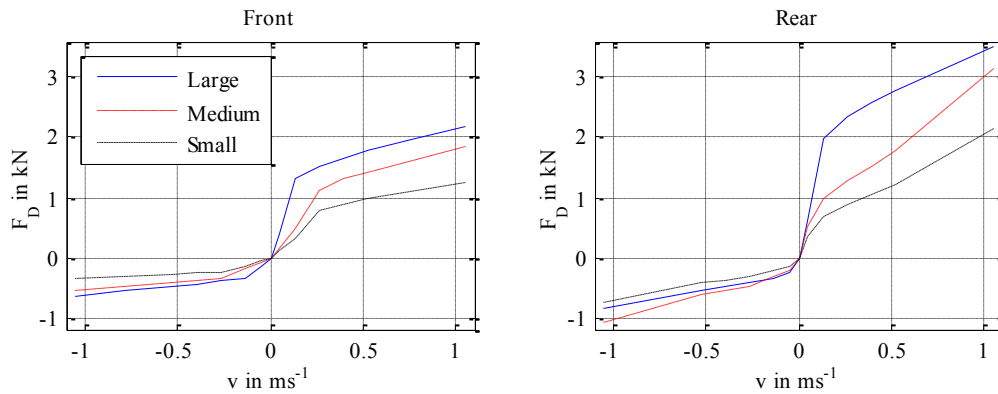


Figure 1 Non-linear damper characteristics in front and rear suspension for the three analysed vehicle types are based on measured data.

Table 2 Analysed vehicle parameters varied in the investigation.

Factor symbol	Vehicle parameter	Variation levels
M	Vehicle mass	$\pm 10\%$
$I_{zz}$	Body yaw moment of inertia	$\pm 10\%$
$I_{yy}$	Body pitch moment of inertia	$\pm 10\%$
$I_{xx}$	Body roll moment of inertia	$\pm 10\%$
L	Wheel base	$\pm 10\%$
$\Lambda$	Longitudinal CG ratio	$\pm 10\%$
K	Vertical CG ratio	$\pm 10\%$
S	Track width	$\pm 10\%$
$C_f$	Front anti-roll bar stiffness	$\pm 10\%$
$C_r$	Rear anti-roll bar stiffness	$\pm 10\%$
V	Velocity	$\pm 10\%$
$F_i$	Location of fault (front, rear)	FL, RL

## Tyre characteristics

The implemented Magic Formula tyre model for combined slip enables the variation of the tyre characteristics. In total, three different factors on the front, the rear and on all wheels have been studied. Longitudinal and lateral direction of the factor has been altered simultaneously; i.e. for the stiffness scaling factors (SF) of the tyre model applies  $\lambda_K = \lambda_{K_x, \kappa} = \lambda_{K_y, \alpha}$ , for the peak friction coefficient SF applies  $\lambda_\mu = \lambda_{\mu_x} = \lambda_{\mu_y}$ , and for the shape SF applies  $\lambda_C = \lambda_{C_x} = \lambda_{C_y}$ . The chosen parameters are varied according to Table 3. The stiffness scaling factors reduce the tyre stiffness for small slip angles around zero, i.e. normal driving conditions. The peak friction coefficient SF reduces the maximum transferable force between road and tyre, while the shape SF changes the complete shape of the tyre curve as seen in Figure 2.

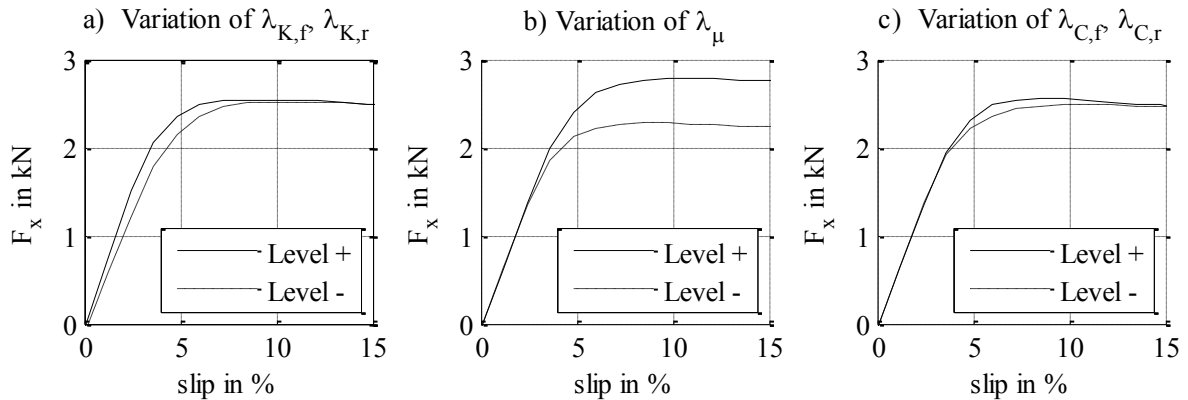


Figure 2 Parameter variation of the longitudinal slip. Variation of the scaling factors for a) stiffness, b) peak friction coefficient and c) shape.

Table 3 Tyre parameters varied in the investigation.

Factor symbol	Tyre parameter	Variation levels
$\lambda_{K,f}$	Stiffness scaling factor (SF), front	$\pm 10\%$
$\lambda_{K,r}$	Stiffness SF, rear	$\pm 10\%$
$\lambda_\mu$	Peak friction coefficient SF	$\pm 10\%$
$\lambda_{C,f}$	Shape SF, front	$\pm 10\%$
$\lambda_{C,r}$	Shape SF, rear	$\pm 10\%$

## Fault characteristics

The chosen fault produces a strong fault torque, which initiates a course deviation of the vehicle without locking the wheel at any time. A locked wheel would change the tyre behaviour towards smaller tyre forces, as seen in Figure 2. In order to exclude the effect of high slip angles on the wheels, the fault characteristics has been chosen in a way that no locked wheel occurred for any of the simulations. The fault's generic character makes typical parameters changes that are relevant in terms of course deviation possible to be analysed, see Table 4. The influence of a fault acting on one wheel compared to a fault acting on one axle is investigated by dividing the induced fault equally on both wheels of the axle. The fault gradient is controlled by a ramping time to reach the fault amplitude. The fault characteristic with the steep gradient develops almost instantly with a ramping time of  $t = 0.02\text{ s}$ , whereas the flat gradient has a ramping time of  $t = 0.2\text{ s}$ . The fault fluctuation is either not activated or has a superimposed sinusoidal signal. Its amplitude is set to 10 % of the fault's amplitude, while its frequency represents a typical 3-phase electric propulsion machine with a high switching frequency; here a frequency of  $f = 100\text{ Hz}$  is chosen.

Table 4 Fault parameters varied in the investigation.

Factor symbol	Tyre parameter	Variation levels
$F_1$	Fault location	Front or rear axle
$F_2$	Number of wheels	One or two wheels
$F_3$	Amplitude of fault	$\pm 10\%$
$F_4$	Fault starting gradient	Steep, flat
$F_5$	Fault fluctuation	On, off
$F_6$	Velocity	$\pm 10\%$

## Evaluation criteria

Three evaluation criteria are chosen to independently analyse longitudinal, lateral and yaw motion of the vehicle. The longitudinal motion is measured by the deviation in travelling speed in x-direction,  $\Delta v_x$ , at 1 s after fault induction. The second criterion is the lateral motion. It is evaluated by the lateral offset,  $\Delta y$ , for the same time instant of 1 s. The yaw stability is measured by the maximum side slip angle on the rear axle,  $\alpha_r$ , that occurs during the first second after fault induction. For more information on the evaluation time, see (5).

## RESULTS AND DISCUSSION

All simulations were conducted for a straight line driving manoeuvre on a dry road with a high friction coefficient of  $\mu = 1$ . The base velocity was set to 80 km/h. Figure 3 displays the longitudinal velocity difference, the lateral offset and the maximum rear slip angle over time for all results of the vehicle parameter analysis for the small vehicle with a front axle fault. Despite the large variation between each result, the characteristic behaviours are clearly seen, e.g. the constant increase of the longitudinal velocity difference due to a constant fault characteristic as well as the delay of the lateral offset due to the inertia and the tyre model. Additionally, the variations and mean values for the evaluation criteria are shown at 1 s after the fault induction.

The FFD results for the vehicle parameters are shown in Figures 4 – 7. Variations and mean values of the three evaluation criteria for all vehicle types and fault locations are found in Figure 4, which gives an indication for the absolute values. Figure 4(a) shows a distinct and linear increase of the  $\Delta v_x$  mean value from  $0.77 \text{ ms}^{-1}$  for the small vehicle to  $1.0 \text{ ms}^{-1}$  for the larger vehicle in both fault locations. The variations show a slight change between the vehicle types and fault locations. An increasing impact on  $\Delta v_x$  for larger vehicle types is found due to their fault torque levels according to the average power ratio. The lateral offset in Figure 4(b) is almost constant for a rear axle fault for all vehicle types, but increases for a front axle fault with a larger vehicle type. Figure 4(c) shows the directional stability with  $\alpha_r$ , which has the highest variation ranging between  $0.6^\circ$  and  $2.0^\circ$ . Mean values increase slightly with a larger vehicle for both fault locations. Due to load transfer caused by the fault, the front axle is more sensitive to a fault and has a higher influence on all evaluation criteria.

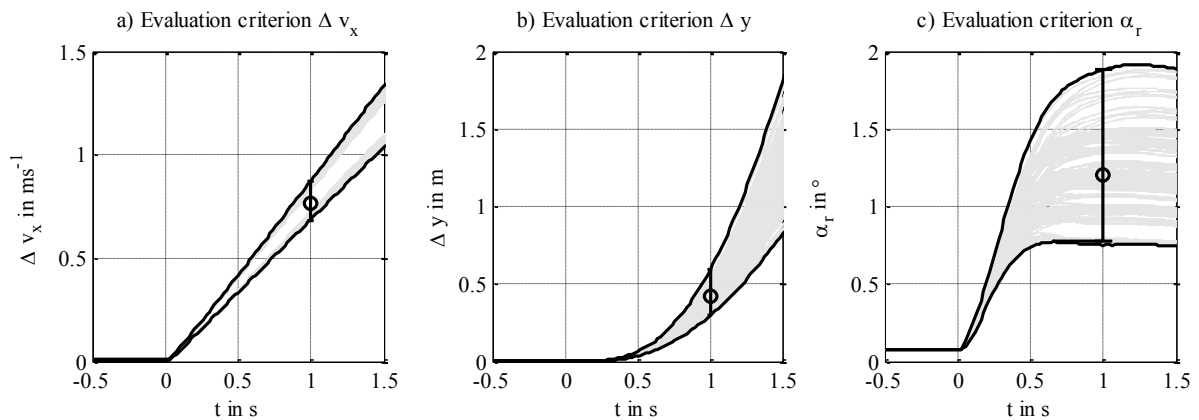


Figure 3 Visualisation of the variations of the vehicle motions: a) longitudinal speed deviation, b) lateral offset and c) maximum rear slip angle after 1s for all results of the small vehicle with front axle fault ( $S_f$ ). Fault induction at  $t = 0 \text{ s}$ .

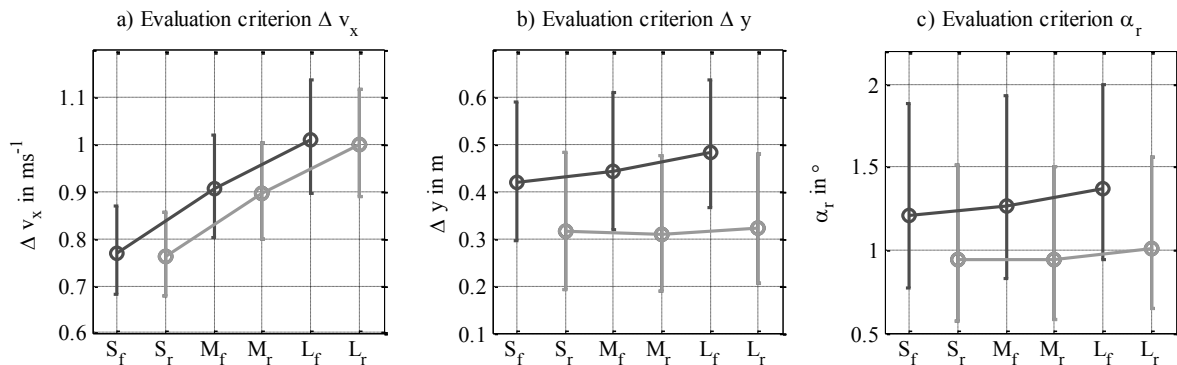


Figure 4 Variation and mean values of all vehicle parameter results for the three evaluation criteria. Note that  $S_f$  here corresponds to the small vehicle with front axle fault described in Figure 3.

In Figure 5 main factor and first-order interaction effects are plotted in descending order of their level of influence on the longitudinal velocity difference  $\Delta v_x$ . For each effect, the three vehicle types and fault locations are plotted with the small vehicle with front axle fault to the left and the large vehicle with rear axle fault to the right. It can be clearly seen that the mass factor has the strongest influence on the longitudinal behaviour. With increasing mass, the longitudinal velocity difference decreases around  $0.2 \text{ ms}^{-1}$  ( $0.72 \text{ kmh}^{-1}$ ) for the large vehicle. This decrease can be explained by the constant fault characteristic. Since the fault is fixed, an increase in vehicle mass results in a reduction of the vehicle deceleration. The factors vehicle velocity, wheel base, track width and longitudinal ratio of centre of gravity are considerably small compared to the factor mass. Interaction effects are negligible as well. Note that all missing main and interaction effect that are not displayed are smaller than the presented ones.

The impact of main and interaction effects on the lateral offset  $\Delta y$  of a vehicle are presented in Figure 6. Most influential factors are vehicle velocity, wheel base, track width, mass and yaw inertia. Vehicle velocity as the most sensitive factor has the expected increase of  $\Delta y$  for the higher velocity. Moreover, a front axle fault has a higher influence on the lateral offset compared to a fault on the rear axle. Besides the expected influence of the vehicle velocity, the lateral offset can be decreased by designing a vehicle with long wheel base, a narrow track width, a higher vehicle mass or higher yaw inertia. Further, moving the longitudinal centre of gravity position to the rear decreases  $\Delta y$  for a fault on the front axle, while the opposite behaviour is shown for a fault on the rear axle. The interaction effects  $M \cdot \Lambda$ ,  $S \cdot V$ ,  $L \cdot S$  and  $J_z \cdot L$  are small and have similar influences on the lateral offset.

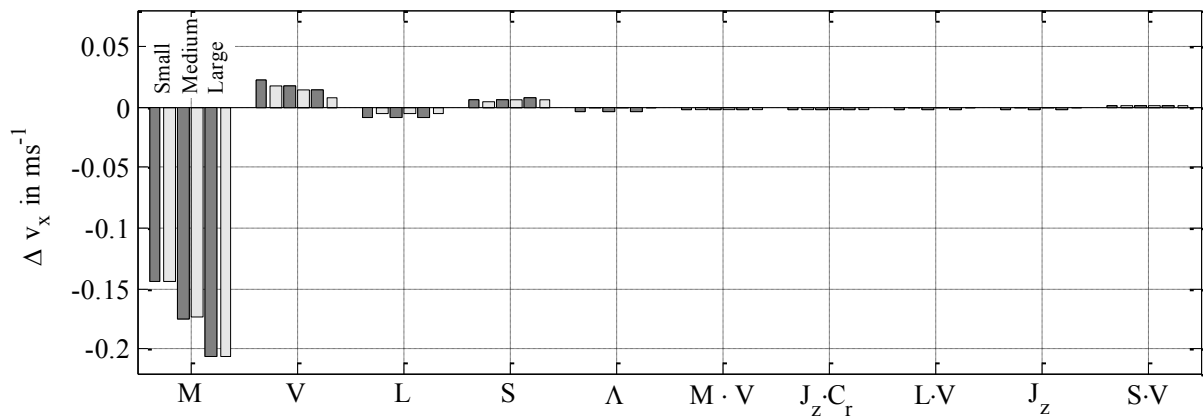


Figure 5 Main and interaction effects of a change in the vehicle parameters for  $\Delta v_x$  after 1 s. (dark/light grey = fault on front/rear axle).

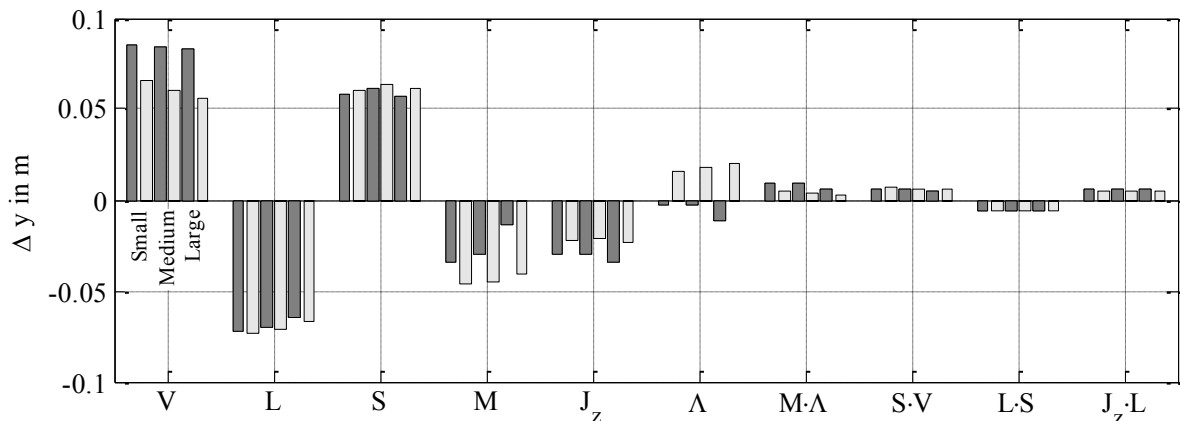


Figure 6 Main and interaction effects of a change in the vehicle parameters for  $\Delta y$  after 1 s. (dark/light grey = fault on front/rear axle).

The effects on the maximum side slip angle on the rear axle  $\alpha_r$  are depicted in Figure 7. The factors with the highest influence are wheel base, vehicle velocity, mass and track width in descending order. Interaction effects are visible for  $M \cdot V$ ,  $J_z \cdot C_r$ ,  $M \cdot \Lambda$  and  $M \cdot L$ . A reduction of  $\alpha_r$ , and thus an improvement on the directional stability of a vehicle, is achieved by a long wheel base, a low velocity, a high mass and a narrow track width. Moving the centre of gravity to the rear also leads to smaller rear side slip angles.

The results for a variation in tyre parameters are shown in Figures 8 – 10. The highest influence on all evaluation criteria is given by the tyre stiffness scaling factor on the rear axle. Longitudinal velocity difference, lateral offset and maximum rear side slip angle decrease with stiffer tyre characteristics on the rear axle. Softer rear

tyres lead to the vehicle braking slightly more due to a higher body slip angle. Therefore,  $\Delta v_x$  is decreasing with stiffer tyres on the rear axle. The effect of higher stiffness on the front axle shows a slight increase of the three criteria on the other hand. The results for the tyre parameters depend also significantly on the fault location. It is clearly shown that a front axle fault has a higher influence on the course deviation. The large vehicle experiences the highest impact of changing tyre properties for all effects, whereas the medium vehicle shows the lowest relative variance. The friction coefficient factor plays a smaller role, which can be attributed to low longitudinal slip values. Thus, high friction utilisation is rarely achieved during the conducted manoeuvre and an effect of this factor is not considerably noticeable here.

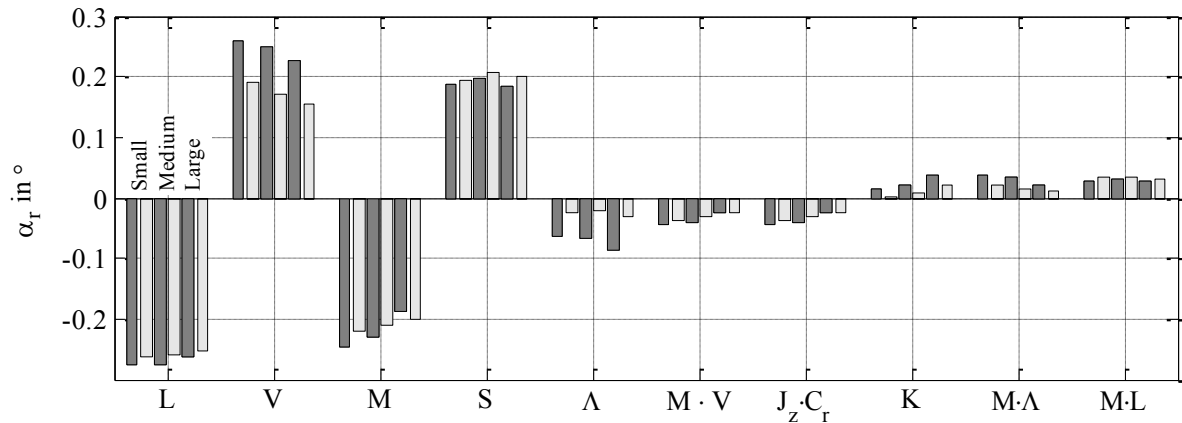


Figure 7 Main and interaction effects of a change in the vehicle parameters for  $\alpha_r$  within 1 s after fault induction. (dark/light grey = fault on front/rear axle).

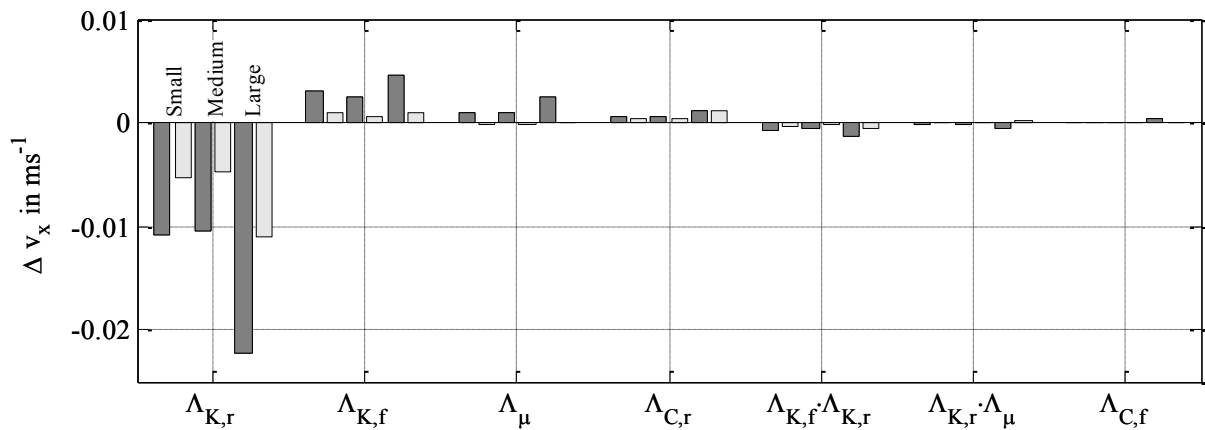


Figure 8 Main and interaction effects of a change in the tyre parameters for  $\Delta v_x$  after 1 s. (dark/light grey = fault on front/rear axle).

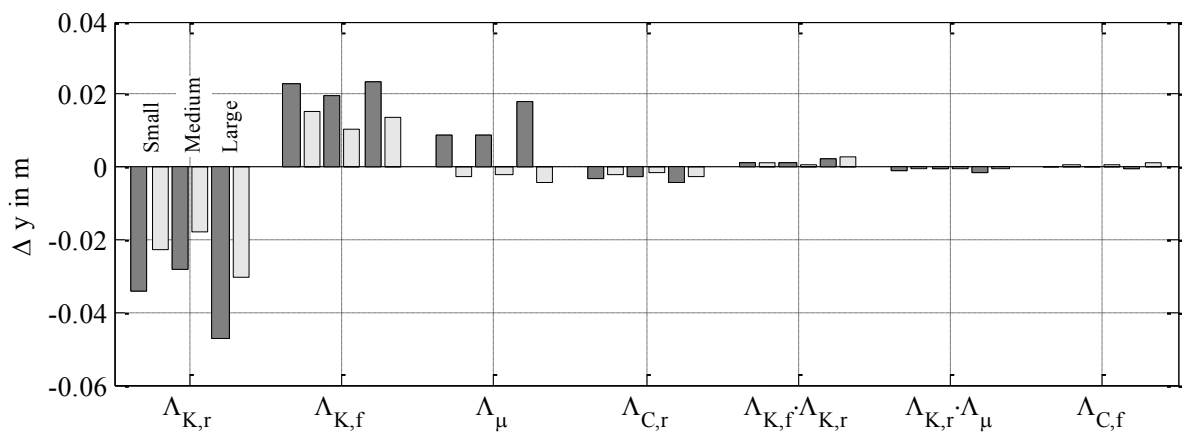


Figure 9 Main and interaction effects of a change in the tyre parameters for  $\Delta y$  after 1 s. (dark/light grey = fault on front/rear axle).

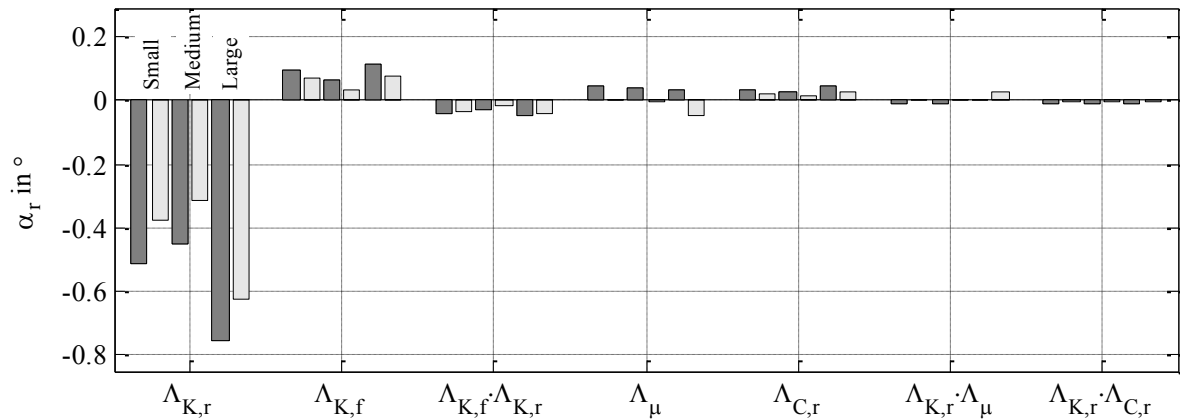


Figure 10 Main and interaction effects of a change in the tyre parameters for  $\alpha_r$  within 1 s after fault induction. (dark/light grey = fault on front/rear axle).

In Figure 11, the results of the six most sensitive main and interaction effects of the fault parameters for all evaluation criteria are shown. The fault location ( $F_1$ ) is integrated in the result plots as it is considered to be part of the fault characteristics. The longitudinal velocity difference increases for most of the factors. The fault amplitude ( $F_3$ ) has the strongest influence, followed by the fault starting gradient ( $F_4$ ) and the number of wheels ( $F_2$ ). On the other hand, the highest impact on the lateral offset and the maximum rear slip angle is caused by the factor number of wheels. It reduces  $\Delta y$  and  $\alpha_r$  because the fault is distributed equally on both wheels of the axle. The large vehicle has a considerably stronger impact for all criteria.

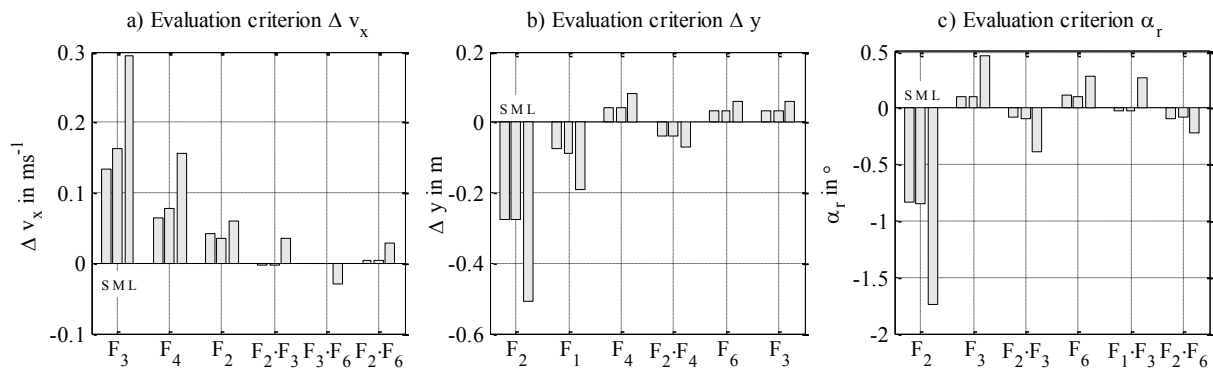


Figure 11 Main and interaction effects of a change in the fault parameters for all three evaluation criteria.

## CONCLUSIONS

The research study presented herein has analysed the effects of different vehicle, tyre and fault parameters on the dynamic behaviour of the vehicle in case of a fault. Based on measured vehicle data, three vehicle types have been investigated to cover a broad spectrum of passenger cars. The applied methodology is based on fractional factorial design and the results are evaluated with three criteria covering longitudinal, lateral and yaw motion of the vehicle. Vehicle parameters of high sensitivity have been found for each criterion. The mass factor is highly relevant for all three motions, while the additional factors wheel base, track width, yaw inertia and vehicle velocity are mainly influencing the lateral and the yaw motion. The tyre parameters are in general less significant than the vehicle parameters. The stiffness factor of the rear axle has a major influence with a reduction of the course deviation for a stiffer tyre. The results for the tyre parameters depend also significantly on the fault location. Due to load transfer caused by the fault, the front axle is more sensitive to a fault and has a higher influence on all evaluation criteria. In general, the fault parameters have a considerably higher influence on the large vehicle type. Important fault parameters are the fault amplitude, the fault starting gradient and the number of wheels with fault. In this study, it was found that the larger vehicle representing a SUV is more sensitive to these types of faults, which can be attributed to the individual fault torque level. To conclude, the result of an electric powertrain fault can result in significant course deviations for all three vehicle types studied.



## REFERENCES

- [1] S.A. Ferguson. The effectiveness of electronic stability control in reducing real-world crashes: a literature review. *Traffic Injury Prevention*, 2007, 8(4):329–338.
- [2] International Energy Agency. Technology roadmap - electric and plug-in hybrid electric vehicles. Study available on [www.iea.org](http://www.iea.org), 2009.
- [3] M. Euchler, T. Bonitz, M. Geyer, and D. Mitte. Evaluation of the dynamic stability of an electric driven vehicle during safety-critical situations in steady state cornering. *VDI-Berichte*, 2009, (2086):316–333.
- [4] M. Jonasson and O. Wallmark. Stability of an electric vehicle with permanent-magnet in-wheel motors during electrical faults. *World Electric Vehicle Journal*, 2007,(1):100–107.
- [5] D. Wanner, L. Drugge, and A. Stensson Trigell. Fault classification method for driving safety of electrified vehicles. accepted for publication in *Vehicle System Dynamics*, 2014.
- [6] C. Zong, C. Liu, H. Zheng, and J. Liu. Fault tolerant control against actuator failures of 4wid/4wis electric vehicles. In *SAE Transactions*, volume 2013-01-0405, 2013.
- [7] D.C. Montgomery. *Design and analysis of experiments*. John Wiley, 1997.
- [8] IPG Automotive GmbH. *CarMaker Reference Manual*, 2011.
- [9] H. Pacejka. *Tyre and vehicle dynamics*. Butterworth-Heinemann Ltd, 2002.
- [10] M. Juhlin. Directional stability of buses under influence of crosswind gusts. *Vehicle System Dynamics*, 2004, (41):93–102.